JOURNAL OF Materials CHEMISTRY

Investigations on thermal reactivity of Si/C/N nanopowders produced by laser aerosol or gas interactions

Djamila Bahloul-Hourlier,* Benoît Doucey, Etienne Laborde and Paul Goursat

SPCTS, UMR CNRS 6638, Faculté des Sciences, 123 avenue A. Thomas, 87 060 LIMOGES, France. E-mail: hourlier@unilim.fr

Received 15th November 2000, Accepted 12th April 2001
First published as an Advance Article on the web 25th June 2001

Ultrafine SiCN particles with various compositions, synthesised by laser pyrolysis in interaction either with gaseous or liquid reactant, were heat treated at temperatures between 300 and1773 K. Thermogravimetric measurements performed under inert (helium) atmosphere, showed that the best thermal stability was exhibited by nanopowders prepared from gaseous precursors (SiH_4, CH_3NH_2, NH_3). Mass spectrometry analysis data revealed that nanopowders derived from a mixture with ammonia and hexamethyldisilazane (HMDS) contained more N–H and C–N groups than those obtained without ammonia. The loss of hydrogen clearly dominated amongst the observed losses in all the examined samples at all temperatures. This study indicates that thermal degradation of such silicon based systems is not a single reaction but the net result of a number of reactions.

The increasing interest in Si/C/N nanocomposite ceramics can be attributed to their wide range of superior properties. These include superplasticity,[1,2] high strength and toughness, as well as excellent high temperature oxidation resistance.[3]

These mechanical performances are influenced by the reduction of the powder particle size to nanometric dimensions (10–100 nm), the chemical composition of the starting powders and the sintering conditions.[4,5] Amongst the various processes that have been reported to produce small sized powders, the CO_2 laser process appears to be one of the most promising. This process, which uses gaseous (SiH_4, CH_3NH_2, C_2H_4)[6–8] or liquid oligosilazane (HMDS: $(CH_3)_3SiNHSi(CH_3)_3$) precursors,[9–11] generally allows control of the composition and dimensions of the particles. These Si/C/N nanopowders may be converted into Si_3N_4/SiC bulk materials by a hot pressing process. Several studies have been devoted to the synthesis of Si/C/N nanopowders and their sintering. Unlike the widely studied organometallic polymer precursors of Si/C/N ceramics,[12–19] only a few studies dealing with the thermal decomposition of these preceramic nanopowders have been reported.[20–24] It is well known that ultrafine powders can undergo structural changes when heated at specific temperatures. This is due to their high surface energy and non-equilibrium phases. A good insight into the species adsorbed onto the surface, the nature of chemical groups present in nanopowders and their reactivity during annealing may be used for further improvement of the colloidal processing, shaping and forming techniques, as well as for optimising the sintering conditions, thus improving the mechanical properties.

The aim of the presented research is to further clarify the effect of synthetic conditions and chemical composition of the Si/C/N preceramic nanopowders on their thermal stability under different atmospheres.

Various experimental techniques TGA/MS (thermogravimetric analysis coupled with mass spectrometry), elemental analysis, and X-ray diffraction were used to analyse the preceramic nanopowders evolution annealing.

Experimental procedure

The Si/C/N preceramic nanopowders produced by laser pyrolysis were analysed. Their fabrication (at the C.E.A., France) has already been described in detail elsewhere.[6,25] Briefly, the laser synthesis of the nanopowders is based on the resonance between the emission of a continuous-wave CO_2 laser at 10.6 μm, and the absorption of either the liquid precursor (hexamethyldisilazane: HMDS) in the form of an aerosol produced by an ultrasonic generator,[10] or gas mixtures containing SiH_4.[6] The two different sources of silicon-reactant, gaseous SiH_4 or liquid HMDS, were used with various gas mixtures (Ar or $Ar + NH_3$) in this work. The addition of NH_3 led to an increase in nitrogen content and to a decrease in free silicon in preceramic nanopowders.

The synthesis conditions and chemical composition of the studied powders with their corresponding designations are reported in Table 1. The quantitative chemical analysis of the nanopowders (performed at Service Central d'Analyse du CNRS, France) enabled the determination of the Si, N, C and O contents in the following manner: the silicon content was determined by ICP (inductive coupled plasma) from an aqueous solution of sodium and/or potassium silicate, resulting from chemical attack on the sample. The carbon content was established by high-temperature combustion and IR spectroscopy of carbon monoxide formed during the pyrolysis of the sample at about 3000 °C, whereas that nitrogen was derived according to a thermal conductivity method. Based on the chemical analysis results, it is possible to determine the chemical composition in the stoichiometric compounds (equilibrium phases: SiO_2, Si_3N_4, SiC) present in the different powders according to the following assumptions: total amount of oxygen is in the form of SiO_2, total amount of nitrogen is bonded to silicon in the form of Si_3N_4 and the remainder of silicon is bonded to carbon in the form of SiC. Free carbon content is calculated from the difference between the total carbon content and the amount of carbon bonded to silicon in the form SiC. These results showed that this synthesis method enabled the variation of the chemical composition by adjusting the process parameters. The studied samples had C/N ratios varying from 0.2 to 2.4. The average particle size was less than 50 nm.

Different analytical techniques were used to investigate the thermal stability of these preceramic nanopowders. Thermogravimetric analysis (TGA) (Netzsch STA 409 apparatus) coupled with a quadripole mass spectrometry (MS) (Quadrex 200, Leybold Heraeus, 70 eV, electron impact) was applied to

 DOI: 10.1039/b009162f

Table 1 Nanopowders chemical composition

Powders	Synthesis precursors	Chemical analysis (weight%)					Atomic ratio	Chemical composition (atom%)					
		Si	C	N	O	Al	C/N	SiO_2	Si_3N_4	SiC	Si	C	N
SiCN40[a]	$SiH_4+CH_3NH_2+NH_3$	58	6	35	1	—	0.2	1	87	8	—	4	—
HMDS40	$HMDS+NH_3+Ar$	51	6	38	5	—	0.2	9	77	—	—	6	8
HMDS10	$HMDS+Ar+NH_3$	52	13	25	10	—	0.6	19	63	7	—	11	—
SiCN0	$SiH_4+CH_3NH_2$	67	13	18	2	—	0.8	4	45	45	6	—	—
HMDS0	$HMDS+Ar$	51	32	15	2	—	2.4	5	37	39	—	19	—

[a]40, 10 and 0 correspond to $\%NH_3$ content ($cm^3\ min^{-1}$) in the reactant synthesis mixture.

simulate the behaviour of powders during the annealing process and to determine the evolved gaseous species.

The experiments were carried out under a dynamic gas atmosphere (helium or nitrogen: 99.999 purity) at a flow rate of 25 $cm^3\ min^{-1}$. The samples (500 mg) were heated in Al_2O_3 crucibles up to 1500 °C, with a heating rate of 10 °C min^{-1}. The crystalline structures of the samples before and after heating were identified by X-ray diffraction (monochromated CuKα radiation).

This study was performed within a National Research Program (GDR 1168), where other groups have analysed the same samples by other characterisation methods such as XPS, EXAFS or ^{29}Si, ^{13}C, MAS NMR and TEM.[26–29]

Results and discussion

Fig. 1 shows a comparison of the measured weight losses during the decomposition of the as-received Si/C/N preceramic nanopowders under a helium flow. At first sight, the results indicate a straightforward dependence of the ceramic yields on the synthesis conditions. Obviously, the overall weight loss was greater for the family of nanopowders derived from the liquid precursor (HMDS) compared to those derived from the gaseous reactant SiH_4. The major weight loss variations mainly evolved at high temperatures ($T>1300$ °C), where extensive degradation of the preceramic nanopowders occurred.

A combined TGA/MS study was used to determine the identity of the species evolved at each step. Only the data corresponding to the sample that exhibited the highest weight loss (HMDS40) will be detailed, as it is not possible, owing to their large number, to illustrate all of the spectra obtained from the analysed powders. However, if differences exist, they will be compared with other samples. The TG/MS analysis of HMDS40 under helium is given in Fig. 2.

On heating from room temperature to 300 °C, the weight loss of 1% corresponds to the simultaneous release of water ($m/z=18$, 17) and ammonia ($m/z=17$, 16, 14). The intensity of the water peaks progressively diminishes with increasing temperature up to approximately 300 °C, whilst ammonia seems to stabilise between 400 and 600 °C, diminishing with further heating. The appearance of two shoulders for the $m/z=17$ peak intensity provides evidence for the occurrence of at least two different reactions.

The departure of H_2O and NH_3 at low temperature (less than 300 °C) may be the consequence of the higher latent reactivity induced by the presence of the condensable ≡Si–NH_2 and Si–OH groups on the preceramic nanopowders, equations (1)–(3).

$$\equiv Si-NH_2 + HO-Si\equiv \rightarrow \equiv Si-NH-Si\equiv + H_2O\uparrow \quad (1)$$

$$\equiv Si-NH_2 + H_2N-Si\equiv \rightarrow \equiv Si-NH-Si\equiv + NH_3\uparrow \quad (2)$$

$$\equiv Si-NH_2 + \equiv Si-NH-Si\equiv \rightarrow \equiv Si-N(-Si\equiv)-Si\equiv + NH_3\uparrow \quad (3)$$

Whilst nitrogen-bridging may take place at low temperatures, the reaction between silanol surface groups is known to take place above 350 °C to form oxygen bridges, equation (4):

$$\equiv Si-OH + HO-Si\equiv \xrightarrow[T>300\,^{\circ}C]{-H_2O} -(Si-O-Si)- \quad (4)$$

Nakamatsu *et al.*[30] proposed the following reaction (5) to explain the simultaneous desorption of both H_2O and NH_3 at low temperatures (around 200 °C).

$$SiONH_4^+ + SiOH \rightarrow Si_2O + H_2O\uparrow + NH_3\uparrow \quad (5)$$

Besides NH_3 and H_2O, some other fragment ions at $m/z=44$, were also detected below 400 °C. The intensities of these peaks are low and thus prevent a detailed characterisation of the original structures.

Between 300 to 900 °C, a second weight loss (3.8%) is attributed to a second release of ammonia ($m/z=17$, 16), which indicates the occurrence of the transamination/condensation reactions (6) which are known to occur during the thermal conversion of polysilazanes.[31]

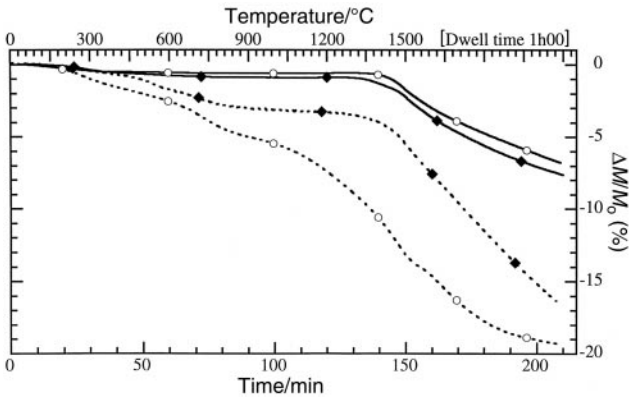

Fig. 1 TG profiles of different nanopowders pyrolysed under a helium flow. —○— SiCN40, —◆— SiCN0, ···◆··· HDMS0, ···○··· HDMS40.

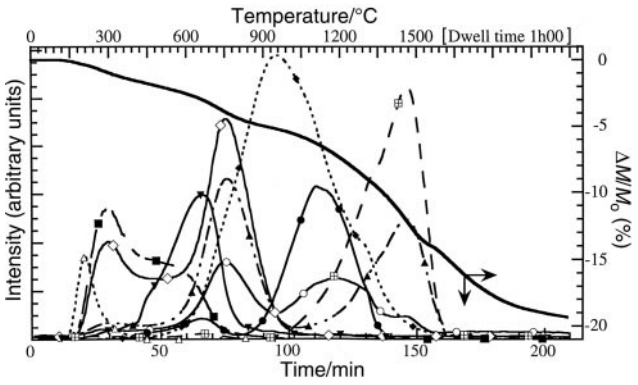

Fig. 2 TG–MS analyses of HDMS40 nanopowder pyrolysed under a helium flow. ···◆··· $m/z=2$, ···▲··· $m/z=14$, · – ·■· – · $m/z=17$, —●— $m/z=27$, —▼— $m/z=41$, —○— $m/z=12$, —◇— $m/z=16$, ···△··· $m/z=18$, · – ·⊞· – · $m/z=28$, —— $\Delta M/M_o$.

$$2(\equiv Si-NH-Si\equiv)+\equiv Si-NH-Si\equiv \rightarrow 2(\equiv Si-N(-Si\equiv)-Si\equiv)+NH_3\uparrow \quad (6)$$

Concomitant with the evolution of NH_3 is the loss of other gases at m/z varying from 42 to 12 (Fig. 3). It is noteworthy that compounds with molecular weights higher than $m/z=42$ were not detected. Observing these peak fragments, one would be tempted to assign them to light hydrocarbons containing no more than three carbon atoms (*i.e.* alkyne, alkene and alkane compounds). However, it should be noted, as the synthesis of this powder was performed with NH_3 gas, which is very reactive towards Si–H, Si–C and C–C bonds, it is most unlikely that hydrocarbon species with two or three carbons in their structure would be formed.[32] Moreover, the comparison of the intensities of the obtained peaks shows that the most intense peak at $m/z=41$ is followed: by descending order in intensity, the peak at $m/z=40$, then $m/z=39$ and finally, by $m/z=42$. No hydrocarbon combination with two or three carbons can lead to such an evolution. It is therefore believed that these fragments may be assigned to R–C≡N species such as CH_3–CN ($m/z=41$, 40, 39, 38), HCN ($m/z=26$, 27) and carboimines like CH_3–CH=NH ($m/z=42$, 28). Further data confirming the assignment of such species will be presented during the analysis of the exhaust gas at high temperatures ($T>900\,^{\circ}C$).

The maximum departure of these species occurred at 600 °C, whereas in the temperature range 600–900 °C the major detected volatile products were methane ($m/z=16$, 15, 14) and H_2 ($m/z=2$). Methane continues to evolve up to 1000 °C, whereas hydrogen evolution occurs over a wider temperature range up to 1500 °C with a maximum loss at about 900 °C.

It is well known that some of these gaseous emissions occur during the thermal conversion of polycarbosilane and polycarbosilazane polymers and have already been described by several authors whereas others are more specific to this type of laser-irradiated powder.

Considering this temperature range, the reactions that describe the thermal decomposition of these materials are those that most probably involve radical mechanisms. There are several potential sources of radical species that can explain the expelled molecules (see equations (7)–(13)).

$$\equiv Si-CN\rightarrow \equiv Si^{\cdot}+{}^{\cdot}CN \quad (7)$$

$$=N-H\rightarrow =N^{\cdot}+{}^{\cdot}H \quad (8)$$

$$\equiv Si-CH_2-Si\equiv \rightarrow Si^{\cdot}+{}^{\cdot}CH_2-Si\equiv \quad (9)$$

$$\equiv Si-CH_2-CN\rightarrow \equiv Si^{\cdot}+{}^{\cdot}CH_2-C\equiv N \quad (10)$$

$$\equiv Si-CH_2-CN\rightarrow \equiv SiCH_2^{\cdot}+{}^{\cdot}C\equiv N \quad (11)$$

$$\equiv Si-CH_2-CN=NH\rightarrow \equiv Si^{\cdot}+{}^{\cdot}CH_2-CH=NH \quad (12)$$

$$\equiv Si-CH_3\rightarrow \equiv Si^{\cdot}+{}^{\cdot}CH_3 \quad (13)$$

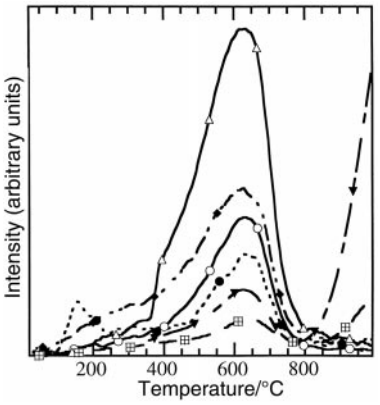

Fig. 3 MS analysis of HDMS40 nanopowder pyrolysed under a helium flow. – – –⊞– – – m/z = 26, —○— m/z = 39, —△— m/z = 41, · – ·▼ · – · m/z = 27, · – ·◆· – · m/z = 40, ···●··· m/z = 42.

For instance, the formation of CH_3–C≡N arises from radical cleavage of Si–CH_2–C≡N leading to the $^{\cdot}CH_2$–C≡N radical, followed by H abstraction and/or radical combination reactions. The formation of the other species can also be explained using this approach.

The C≡N groups do not appear in the initial structure of HMDS precursors, and seem to have been formed during the synthetic procedure. This is confirmed by Rice's studies[9] on the laser induced dissociation of the HMDS molecule in the gas phase under argon. The analysis of gases of the processing chamber indicates the presence of other species and, in particular, HCN and hydrocarbons.

Thus, it is not surprising that, as the synthesis was carried out in the presence of NH_3, the concentration of –C≡N or aminated groups giving HCN and RCN species should increase at the expense of C–C groups, pertaining to light hydrocarbon species. Indeed, the reaction of carbon or hydrocarbon compounds with ammonia has been well described elsewhere, with HCN being the resulting product and no evidence of hydrocarbons being observed.[15,32]

Above 900 °C, a significant weight loss was observed. This was accompanied by the increased evolution of the TGA curve shape. Between 900 and 1400 °C, besides H_2 evolution, the major gaseous decomposition product was unambiguously ascribed to HCN at $m/z=26$, 27. This exhaust gas supports the description given above concerning the assignment of HCN and aminated species to the signals at between m/z 42 and 12. This result accords well with the chemical analysis results of the sample HMDS40, as shown in Table 1. It can also be observed that an excess of nitrogen and carbon are obtained assuming that only equilibrium phases SiO_2, SiC, Si_3N_4 and C are present in the as-prepared powders (rule of mixture calculations). Furthermore, the short-range atomic structure description of the same Si/C/N nanopowders by X-ray absorption spectroscopy reveals the presence of C–N bonds in the amorphous network.[33] A structural model has been proposed,[29] where mixed tetrahedral SiC_xN_{4-x} are randomly linked through C–N bonds. The removal of HCN at high temperature is a further proof that CN groups are not only pendant groups, as observed for temperatures $T<900\,^{\circ}C$ or acting as radical scavenger/quenchers under the experimental conditions employed in the synthesis process, but occur as branching groups to probably mixed tetrahedra SiC_xN_y. Homolytic cleavages of C–N bonds between two mixed tetrahedra of silicon require more energy in comparison to those at chain ends.

Parallel to the evolution of HCN gas is the loss of N_2 ($m/z=28$, 14) up to the temperature limit of the experiment (1500 °C), whereas CO loss ($m/z=28$, 12) begins at 1450 °C in minor amounts (comparison of ions at $m/z=12$ for CO and $m/z=14$ for N_2). At 1500 °C, despite the significant weight loss, the intensity of N_2 diminishes rapidly whilst some traces of CO are still detected by MS during isothermal holding. Interestingly, at 1500 °C, we observe that the mass continues to decrease with increasing duration of holding, even though no species can be detected by MS in quantities large enough to account for this continued weight loss. It is believed that this weight loss in the TGA curve is due to compounds such as SiO which, owing to the rapid condensation in cold parts of the apparatus, may not have been detected by MS. This viewpoint is supported by the deposition of SiO as a wool-like product on many parts of the apparatus, leading eventually to the breaking of the platinum-based thermocouple.

The most probable chemical reactions in the Si/C/N/O system, involving the evolution of volatile species and producing an important weight loss, can be described in two steps. First, decomposition of the quaternary $SiC_xN_yO_z$ phase leads to the formation of an intermediate ternary oxynitride solid phase $Si_xN_yO_z$ and the simultaneous release of SiO, CO and N_2, the gas detected to the greatest degree by mass spectrometry.

Secondly, during holding at 1500 °C, the oxynitride phase $Si_xN_yO_z$ then undergoes decomposition in which gaseous N_2, Si(l, v) and SiO evolve and the solid phase is produced according to reaction (14):

$$\begin{array}{l} SiN_xO_yC_z \longrightarrow Si_3N_4 + SiO\uparrow + N_2\uparrow + Si(l,v) \\ \qquad\qquad \searrow \quad \nearrow \\ \qquad\qquad Si_xN_yO_z + N_2\uparrow + CO\uparrow + SiO\uparrow \end{array} \qquad (14)$$

The best known ternary oxynitride phase is Si_2N_2O. Although several investigators have reported on the thermal decomposition of Si_2N_2O, no mechanism has yet been clearly established. This is due to some of the following experimental difficulties: (a) the irreproducibility of experiments, (b) the error in the determination of the weight loss which sometimes does not represent the real value of mass loss, due to condensation of SiO species on the rod attaching the crucible to the balance, (c) progressive clogging of the aperture of the tube furnace and capillary for admission of gas to the mass spectrometer, owing to the deposition of SiO and (d) rupture of the thermocouple, preventing subsequent experiments. The majority of decomposition reactions of Si_2N_2O involve the simultaneous release of the volatile species SiO(g) and N_2(g). Our analysis revealed that, after 10 minutes hold at 1500 °C, no gas species are detected by mass spectrometry, despite the continued weight loss observed by thermogravimetric analysis. It may be assumed that, as the HMDS40 powder has been synthesised with ammonia as a reactant, a significant number of SiN_4 sites are present and the amount of carbon in the powder is low. Taking into account our previous observations, it is thus hypothesised that the oxynitride SiN_xO_y resulting from the decomposition of oxycarbonitride phase $SiN_xO_yC_z$ coexists with SiN_4 sites initially present in the material. Hence as the duration of heating is increased, the oxynitride phase degrades to promote the SiO evolution in greater quantity, whilst the two other species Si(l, v) and N_2 interact on the SiN_4 sites to give better organised Si_3N_4, as illustrated by X-ray diffraction, Fig. 4.

Rocabois *et al.*[34,35] used Knudsen effusion mass spectrometry to study the thermal degradation of several silicon based systems, binary, ternary and even quaternary ones, Si/C/N/O.

The authors stressed that the thermal degradation of silicon-based materials is much less pronounced than predicted by thermodynamics, and that their vaporisation is hindered and related to the different evaporation coefficients of each species. Moreover, the grain size, chemical composition, surface of contacts or interfaces during vaporisation may play an important role in the degradation of various phases. As the nanopowder examined in this study is initially amorphous as shown by X-ray diffraction (Fig. 4), we can postulate that the number of surface contacts is high, and thus the degradation of the material is more homogeneous. By admitting, as suggested by Rocabois *et al.*,[36] that the evaporation coefficient of N_2 is low compared with that of SiO, the two concomitant reactions, decomposition of the oxynitride phase releasing SiO, Si (l, v), N_2 and the reaction of the two latter gaseous species, on initially present SiN_4 sites, leading to Si_3N_4 formation by epitaxial growth, are expected.

Major differences in thermal behaviour of preceramic nanopowders

The results show the major differences between the nanopowders synthesised from the same HMDS precursor with (HMDS40 and HMDS10) or without (HMDS0) ammonia, respectively. The elemental analysis of these powders confirmed that when ammonia was used during synthesis, the C/N ratio decreased. The diminution of carbon also depended on the concentration of NH_3 in the reactant gas mixture. Moreover, during the heat treatment of the powders, the mass spectrometry analysis also confirmed that the powders synthesised in presence of ammonia contained more N–X bonds (X = H, C, Si). Indeed, the evolution of ammonia at $m/z = 17$ (Fig. 5) occurs over a wide temperature range and is characterised by two waves, in the case of HMDS40 and HMDS10, whereas for HMDS0, it exhibits only one narrow wave up to 300 °C. When analysing the HMDS0 powder between 400 and 700 °C, the MS spectra (Fig. 6) revealed the loss of silicon-containing species at $m/z = 73$, 59, 45, 44, 30, suggesting the formation of $(CH_3)_{x\leqslant 4}Si$, whereas for HMDS40 and HMDS10, species with $m/z > 42$ have not been detected. In view of the abundance of such organosilicon species, it seems that under the

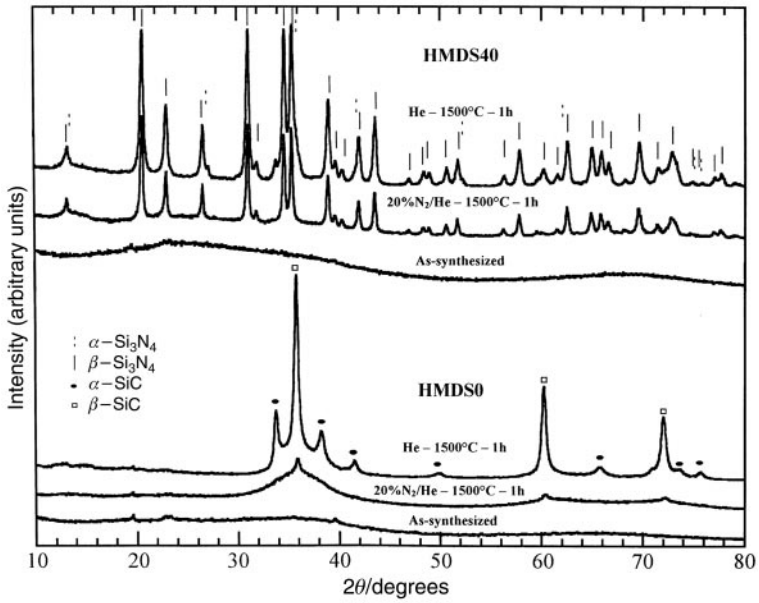

Fig. 4 XRD patterns of nanoparticles pyrolysed under a reactive (20% N_2/He) and inert (He) atmosphere.

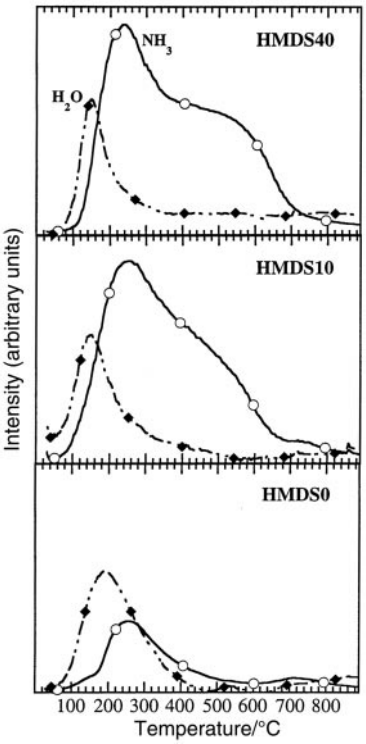

Fig. 5 MS analysis of HMDS nanopowders pyrolysed under a helium flow. —○— $m/z = 17$, ···◆— $m/z = 18$.

experimental conditions used during the synthesis, the laser interaction with HMDS does not induce full atomization of the molecular structure. NH_3 proves to be more reactive toward Si–C, leading to the amination of silicon and carbon sites and is the primary reason for the formation of nitrogen-rich powders.

It can be seen above 800 °C, that HCN is evolved in larger quantities from preceramic powders prepared in the presence of NH_3 during the laser-synthesis process, compared to those prepared without ammonia.

It can also be noted, that as the temperature increases ($T > 1200$ °C) the release of N_2 and CO for carbon-rich powder

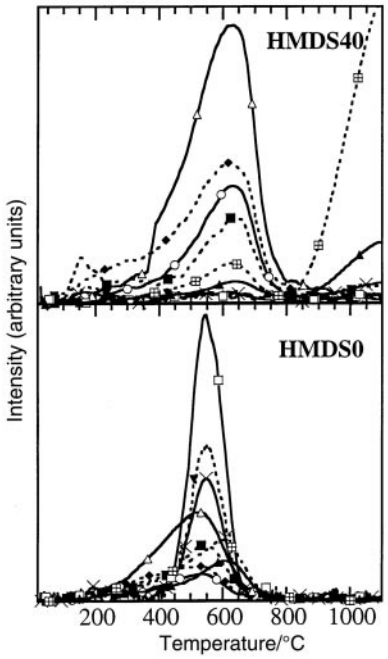

Fig. 6 MS analysis of HMDS nanopowders pyrolysed under a helium flow. —○— $m/z = 39$, —△— $m/z = 41$, —×— $m/z = 43$, —□— $m/z = 73$, ···◆··· $m/z = 40$, ···■··· $m/z = 42$, ···▼··· $m/z = 45$, —▲— $m/z = 26$, ···⊞··· $m/z = 27$.

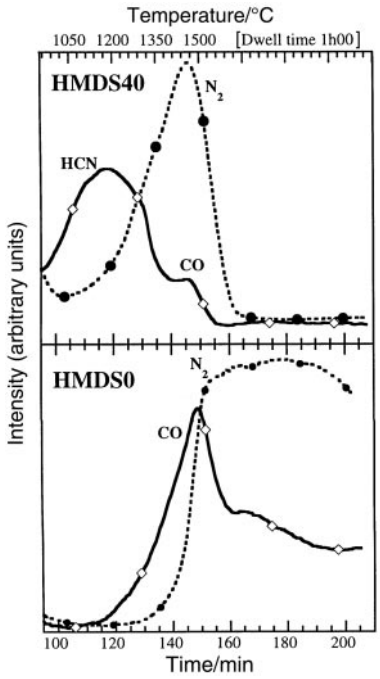

Fig. 7 MS analysis of HMDS nanopowders pyrolysed under a helium flow. ···●··· $m/z = 14$, —◇— $m/z = 12$.

HMDS0 and nitrogen-rich powder HMDS40 is different (Fig. 7). Indeed, the departure of N_2 and CO takes place during the complete thermal cycle for HMDS0, whereas no gas is detected after 10 minutes at 1500 °C for HMDS40 nitrogen-rich powder. This suggests that the thermal degradation of these two nanopowders proceeds according to different reaction paths and depends on the chemical composition and also on the structure of the materials.

The CO response for the carbon-rich powder HMDS0 was not monomodal, indicating that the process involves more than one reaction. The oxynitride intermediate phase suggested for a nitrogen-rich powder in reaction (14) can not be formed, as an excess of carbon is present. According to a previously discussed thermal decomposition of a silicon carbonitride material, containing free carbon phase and derived from polysilazane precursors, the degradation of carbon-rich nanopowders may be described by reaction (15):[17]

$$SiC_xN_yO_z + C_{free} \longrightarrow SiC + CO\uparrow + N_2\uparrow \quad \text{via } Si(l,v) \qquad (15)$$

The loss of CO starts at about 1150 °C, whereas the release of N_2 is observed from 1300 °C. This can be explained in analogy to the reaction (16) observed in the solid phase by the carboreduction of Si–O bonds by excess carbon.

$$SiO_2 + 3C \rightarrow SiC + 2CO\uparrow \qquad (16)$$

In an analogous fashion the large amount of N_2 evolved during the holding time at 1500 °C can be accounted for by the reaction of Si–N and carbon (reaction (17)):

$$Si_3N_4 + 3C \rightarrow 3SiC + 2N_2\uparrow \qquad (17)$$

Several authors[36,37] have suggested that this reaction is inhibited when a SiC layer is formed on the carbon surface. This causes the system to shift to another system equivalent to SiC/Si_3N_4 and the excess loss of N_2 would be suspected from the direct decomposition of Si_3N_4 following reaction (18):

$$Si_3N_4 \rightarrow 2N_2\uparrow + 3Si \qquad (18)$$

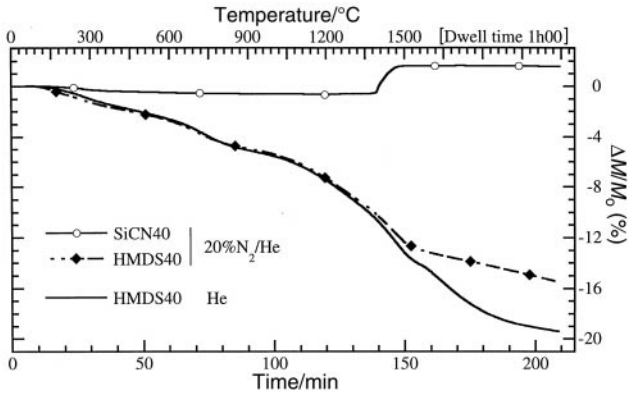

Fig. 8 TG profiles of different nanoparticles pyrolysed under a 20%N_2/He flow.

Table 2 Nanopowders weight loss according to the heat treatment atmosphere

	Weight loss $\Delta M/M_o$ (%)			
Treatment atmosphere	SiCN0	SiCN40	HMDS0	HMDS40
He	−7.7	−6.8	−16.3	−19.3
20%N_2/He	+6.1	+1.3	−6.2	−15.5

As the experimental procedure of heat treatment is the same for all the powders, we should expect that nitrogen enriched powders generate more N_2 than the carbon enriched ones, since they contain more Si_3N_4 phase. However, this was not the case. Consequently, the decomposition of Si_3N_4 is not able to offer an explanation for the evolution of nitrogen observed. Furthermore, the powder samples after heat treatment showed no evidence of the presence of elemental silicon when examined by XRD (Fig. 4). SiC is one of the main compounds in the samples derived from carbon-rich HMDS0 powder heated at 1500 °C under helium. The small emission of CO during the holding time can be attributed to reactions (19) and (20):

$$2SiO_2 + SiC \rightarrow 3SiO\uparrow + CO\uparrow \quad (19)$$

$$SiO + 2C \rightarrow SiC + CO\uparrow \quad (20)$$

Our system suggests that the SiC derived from the reaction of Si_3N_4 with carbon (equation (17)) may be consumed by SiO_2, following reaction (19), which, in turn, releases the embedded carbon particles and consequently allows the reaction (17) to continue and produce gaseous N_2.

Thermal behavior of nanopowders under nitrogen atmosphere

The purpose of this study is to determine whether the heat treatment under nitrogen could prevent the decomposition of SiCN, seen to occur under helium. The structural evolution of various nanopowders was observed as a function of heat treatment temperature and time, under a nitrogen atmosphere.

The resulting curves in Fig. 8, representing the nanopowders that have the same ratio C/N = 0.2, show that below 1300 °C the weight losses are nearly identical regardless of the nature of the atmosphere (N_2 or He). The main gases detected by MS are attributed to the same species as those detected under helium.

In contrast, above 1400 °C, comparison of the variation of mass is noticeably lower under nitrogen than helium, as is shown for the HMDS40 sample. These differences are more pronounced for SiCN nanopowders formed from only gaseous reactants ($SiH_4 + CH_3NH_2 + NH_3$), as shown in the data, Table 2.

The volatile species evolved are similar to those derived under helium with a majority of CO but to a lesser degree. Furthermore, it can be seen, Fig. 9, that the variation of mass remarkably decreases with increasing the nitrogen partial pressure. These results suggest that carbothermal nitridation reactions take place at high temperature under nitrogen according to equation (21):

$$SiN_xO_yC_z + N_2 \rightarrow Si_3N_4 + \text{gaseous species}(CO + SiO) \quad (21)$$

For carbon rich powders containing more SiC phase, the nitriding process is also possible *via* reaction (22)

$$3SiC + 2N_2\uparrow \leftrightarrow Si_3N_4 + 3C \quad (22)$$

The weight gain, particularly observed for SiCN synthesised from gaseous reactants, can be attributed to the nitridation reaction of excess elemental silicon detected by XRD.[23] According to the α- or β-Si_3N_4 content calculated from XRD patterns of heat treated powders, the nitridation reaction leads to the preferential formation of the α phase. This could be

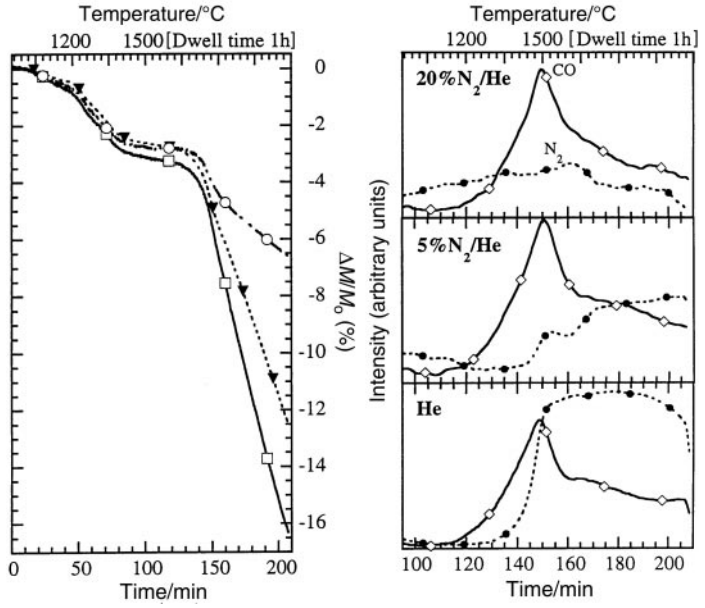

Fig. 9 TG–MS analysis of HMDS0 pyrolysed under different atmospheres. —□— He, ··· ▼ ··· 5% N_2/He, · – · ○ · – · 20% N_2/He, —◇— m/z = 12, ··· ● ··· m/z = 14.

explained by an oversaturation in nitrogen arising from the nitrogen atmosphere, resulting in the crystallisation of the less ordered α phase. Meanwhile, the more ordered and stable β silicon nitride phase is preferentially formed during annealing under the inert helium atmosphere.

The influence of the silicon precursors origin on the chemical composition and thermal stability

The use of a silicon gas source such as SiH_4 led to nanopowders of a more stable nature in terms of temperature, undoubtedly due to their higher degree of crystallisation as revealed by XRD. The formation of CN bonds does not seem favoured when SiH_4 is used. However, contrary to the HMDS powders, the use of silane (SiH_4) generates an excess of elemental silicon within the powders, which will be made profitable during sintering under nitrogen.

Conclusion

This study indicates that the relative atomic concentrations of Si, C and N in Si/C/N nanopowders are primarily influenced by the types of carrier gases used for the laser synthesis process. Residual functionalities, C–H, N–H and Si–H bonds, will still be present as supported by the identification of the volatile species by MS. The study of heat treatment of such a silicon based system indicates that thermal degradation is not a single reaction but the net result of sequential reactions. The difference in thermal behaviour is attributed to variations in the preceramic structure. Taking into consideration the gases detected during our investigation and comparing them with similar results reported by other research groups,[7,9] we suggest that thermal decomposition analysis of the preceramic nanopowders enables one to identify the powder synthesis process. A potential advantage of laser-driven synthesis of refractory materials from liquid reactants is the ability to introduce additives and co-reactants (*e.g.* sintering aids) into the system in a truly homogeneous fashion.[38]

Acknowledgements

We acknowledge M. Cauchetier and his colleagues for the synthesis of nanopowders (CEA Saclay-DSM-DRECAM-SPAM, 91 191 Gif/Yvette, France).

References

1 F. Wakai, S. Sakaguchi and Y. Matsuno, *Adv. Ceram. Mater.*, 1986, **1**, 259.
2 M. Mayne, T. Rouxel, D. Bahloul-Hourlier and J.-L. Besson, *J. Eur. Ceram. Soc.*, 1998, **18**, 1985.
3 T. Hirano, K. Niihara, T. Ohji and F. Wakai, *J. Mater. Sci. Lett.*, 1996, **15**, 505.
4 G. Sasaki, H. Nakase, K. Suganuma, T. Fujita and K. Niihara, *J. Ceram. Soc. Jpn.*, 1992, **100**(4), 536.
5 J.-J. Park, O. Komura, A. Yamakawa and K. Niihara, *J. Am. Ceram. Soc.*, 1998, **81**(9), 2253.
6 M. Cauchetier, O. Croix, M. Luce, M. I. Baraton, T. Merle and P. Quintard, *J. Eur. Ceram. Soc.*, 1991, **8**, 215.
7 E. Borsella, S. Botti, R. Fantoni, R. Alexandrescu, I. Morjan, C. Popescu, T. Dikonimos-Makris and R. Giorgi, *J. Mater. Res.*, 1992, **7**(8), 2257.
8 M. Suzuki, Y. Maniette, Y. Nakata and T. Okutani, *J. Am. Ceram. Soc.*, 1993, **76**(5), 1195.
9 G. W. Rice, *J. Am. Ceram. Soc.*, 1986, **69**(8), C183.
10 M. Cauchetier, O. Croix, N. Herlin and M. Luce, *J. Am. Ceram. Soc.*, 1994, **77**(4), 993.
11 Y.-L. Li, Y. Liang, F. Zheng and Z.-Q. Hu, *Mater. Sci. Eng.*, 1994, **A174**, L23.
12 H. H. Han, D. A. Lindquist, J. S. Haggerty and D. Seyferth, *Chem. Mater.*, 1992, **4**, 705.
13 Y. D. Blum, K. B. Schwartz and R. M. Laine, *J. Mater. Sci.*, 1989, **24**, 1707.
14 G. T. Burns, T. P. Angelotti, L. F. Hannemen, G. Chandra and J. A. Moore, *J. Mater. Sci.*, 1987, **27**, 4651.
15 R. J. P. Corriu, D. Leclercq, P. H. Mutin and A. Vioux, *Chem. Mater.*, 1992, **4**, 711.
16 W. R. Schmidt, P. S. Marchetti, L. V. Interrante, W. J. Hurley, R. H. Lewis, R. H. Doremus and G. E. Maciel, *Chem. Mater.*, 1992, **4**, 937.
17 D. Bahloul, M. Pereira and P. Goursat, *J. Am. Ceram. Soc.*, 1993, **76**(5), 1163.
18 A. Lavedrine, D. Bahloul, P. Goursat, N. S. Choong Kwet Yive, R. J. P. Corriu, D. Leclercq, P. H. Mutin and A. Vioux, *J. Eur. Ceram. Soc.*, 1991, **8**, 221.
19 D. Bahloul, M. Pereira and C. Gerardin, *J. Mater. Chem.*, 1997, **7**(1), 109.
20 R. Giorgi, S. Turtu, G. Zappa, E. Borsella, S. Botti, M. C. Cesile and S. Martelli, *Appl. Surf. Sci.*, 1996, **93**, 101.
21 M. Suzuki, Y. Hasegawa, M. Aizawa, Y. Nakata and T. Okutani, *J. Am. Ceram. Soc.*, 1995, **78**(1), 83.
22 E. Borsella, S. Botti, S. Martelli, R. Alexandrescu, M. C. Cesile, A. Nesterenko, R. Giorgi, S. Turtu and G. Zappa, *Silicates Ind.*, 1997, **1–2**, 3.
23 M. Mayne, D. Balhoul-Hourlier, B. Doucey, P. Goursat, M. Cauchetier and N. Herlin, *J. Eur. Ceram. Soc.*, 1998, **18**, 1187.
24 Z. W. Pan, S. Xie, G. Wang, H. L. Li and L. T. Zhang, *J. Mater. Sci.*, 1999, **34**, 3047.
25 J. S. Haggerty and W. R. Cannon, *Laser-Induced Chemical Processes*, ed. J. I. Steinfeld, Plenum Press, New York, 1981, ch. 3.
26 E. Musset, PhD thesis, Université Paris XI, 1995.
27 *Nanostructured Silicon-based Powders and Composites*, ed. A. P. Legrand and C. Sénémaud, Gordon and Breach, New York, 2001, in press.
28 Y. El Kortobi, PhD thesis, Université Paris VI, France, 1998.
29 F. Ténégal, PhD thesis, Université Paris VII, France, 1998.
30 T. Nakamatsu, N. Saito, C. Ishizaki and K. Ishizaki, *J. Eur. Ceram. Soc.*, 1998, **18**, 1273.
31 M. Pereira, PhD thesis, Université de Limoges, France, 1994.
32 F. K Van Dijen and J. Pluijmakers, *J. Eur. Ceram. Soc.*, 1989, **5**, 385.
33 F. Ténégal, A.-M. Flank and N. Herlin, *Phys. Rev. B*, 1996, **54**(17), 12029.
34 P. Rocabois, PhD Thesis, I.N.P.G., France, 1993.
35 P. Rocabois, C. Chatillon and C. Bernard, *J. Am. Ceram. Soc.*, 1996, **79**(5), 1351.
36 P. Rocabois, C. Chatillon and C. Bernard, *J. Am. Ceram. Soc.*, 1996, **79**(5), 1361.
37 N. S. Jacobson, K. N. Lee and D. S. Fox, *J. Am. Ceram. Soc.*, 1992, **75**(6), 1603.
38 M. Cauchetier, X. Armand, N. Herlin, M. Mayne, S. Fusil and E. Lefevre, *J. Mater. Sci.*, 1999, **34**(21), 5257.